A review of high contrast imaging modes for METIS

Matthew A. Kenworthy[a], Olivier Absil[b], Brunella Carlomagno[b], Tibor Agócs[c], Emiel H. Por[a], Bernhard Brandl[a], and Frans Snik[a]

[a]Leiden Observatory, Leiden University, P.O. Box 9513, 2300 RA Leiden, The Netherlands
[b]Space sciences, Technologies, and Astrophysics Research (STAR) Institute, Université de Liège, 19c allée du Six Août, B-4000 Sart Tilman, Belgium
[c]NOVA Optical Infrared Instrumentation Group at ASTRON, P.O. Box 2, 7990 AA, The Netherlands

ABSTRACT

The Mid-infrared E-ELT Imager and Spectrograph (METIS) for the European Extremely Large Telescope (E-ELT) consists of diffraction-limited imagers that cover 3 to 14 microns with medium resolution ($R \sim 5000$) long slit spectroscopy, and an integral field spectrograph for high spectral resolution spectroscopy ($R \sim 100,000$) over the L and M bands. We present our approach for high contrast imaging with METIS, covering diffraction suppression with coronagraphs, the removal of residual aberrations using QACITS and Phase Sorting Interferometry (PSI), and simulations demonstrating the expected contrast.

Keywords: ELT, high contrast imaging, coronagraphs, thermal IR

1. INTRODUCTION

This paper details the high contrast imaging (HCI) modes of METIS, used in the cases where noise caused by the diffraction halo of a star is the dominant noise source for a given region of the science image. HCI is used mostly for the direct imaging and characterisation of faint point sources and extended structures around stars, typically low masss, stars, thermally self luminous exoplanets, circumstellar disks and the structure therein. The HCI modes for METIS cover both imaging (for detection, photometric variability and characterisation) and spectroscopy (for atmospheric modeling, chemical characterisation and orbital dynamics). The coronagraphs are used for imaging in the L, M and N bands, and for the high spectral resolution mode in the L/M band integral field unit, and all have small inner working angles (IWAs) that exploit the large aperture of the Extremely Large Telescope and extreme performance of the adaptive optics system. We describe the optical layout and location of the optical components for the HCI modes along with the expected coronagraphic performances.

2. LAYOUT

The detailed optical design of METIS is described in REF Tibor paper. We represent the optics of METIS with a "Tube map" of the optical components relevant to the Tube diagram, observing mode names and optics. Figure 1 shows this schematic, starting at the left with the ELT primary mirror M1. The primary mirror may have unphased segments that result in an incomplete pupil, due to the requirement of replacing and recoating mirrors during the operation of the telescope, the primary mirror may have unphased segments that result in an incomplete pupil. Adaptive correction is provided by the adaptive mirror M4, which has actuators used to deform the mirror surface in response to commands from the adaptive optics control system. Further mirrors then pass the light into the METIS dewar, and form a focal plane image at ELT-FP1. The first set of reimaging optics in METIS are referred to as Common Fore Optics (CFO) through which the telescope beam is transmitted. From this point on all optics are in vacuum at cryogenic temperatures. The focal plane is reimaged to a cold stop at CFO-PP1 where a mechanical wheel can place different masks into the beam. A K mirror acts as the derotator, rotating the observed sky image with respect to the downstream optics. The CFO forms a focal plane image at CFO-FP1 and then a dichroic reflects light shorter than 3 microns into the Wavefront Sensor optical train and

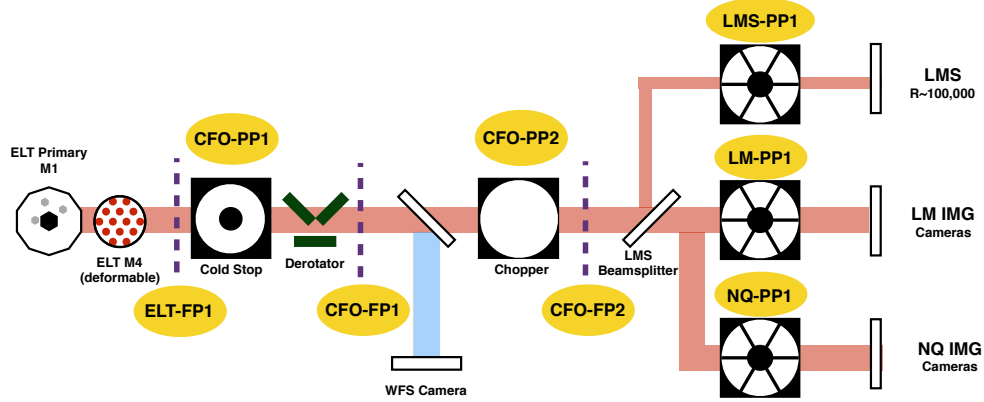E-mail: kenworthy@strw.leidenuniv.nl, Telephone: +31 (0) 71 527 8455

Figure 1. The schematic map of METIS showing the location and names of the pupil and focal planes used in HCI, and the names of the optics in the light path.

all the longer wavelength light is then reimaged into a pupil image at CFO-PP2 where a fst cryogenic chopping mirror provides the ability for rapid beam steering and chopping.

A second focal plane is formed at CFO-PP2 and then a dichroic splits light between two camera channels, the LM IMG camera and the NQ IMG camera. After the dichroic there is a pupil location in each of the camera channels, LM-PP1 and NQ-PP1, before the final focal plane images are formed at LM IMG and NQ IMG.

3. THE CORONAGRAPHS

Two coronagraphic architectures are in the baseline design for METIS - a Vortex coronagraph realised with an Annular Groove Phase Mask (AGPM) and matching Lyot mask, which can be additionally combined with a Ring Apodizer (RA) in a pupil plane to form a Ring Apodized Vortex Coronagraph (RAVC). The RAVC is sensitive to tip tilt errors that are above the bandwidth of the adaptive optics (AO) system, but it allows for a wide search space around a target star in to an IWA of 1.1 λ/D. Atmospheric dispersion increases with increasing zenith angle of the stellar target, and the resulant dispersion of the star PSF with wavelength results in degraded performance of the VC. To compensate for this, a series of atmospheric dispersion correctors, each with a predetermined and fixed atomsphreic dispersion anre present in a pupil wheel next to the CFO-PP1. These provide adequate atmospheric dispersion compensation to ensure minimal degradation of VC performance.

A pupil plane only coronagraph called the Apodizing Phase Plate (APP) coronagraph is realised in METIS as a grating vector Apodizing Phase Plate (gvAPP) coronagraph, enabling lower throughput and larger IWA (typically $1.5 - 2.0\lambda/D$) but more reliable coronagraphic performance and enabling beam switching during observation cycles.

3.1 The grating vector Apodizing Phase Plate coronagraphs

Figure 2 shows the locations of gvAPP coronagraphs in METIS. The gvAPP consists of one optic in one of the pupil planes for METIS. The LM band imager has one gvAPP at the IMG-PP2 location, splitting the PSF of the star into three PSFs, two PSFs with a dark 'D' shaped region on opposite sides of it. Each PSF contains about 49% of the total flux of the star. A third PSF, called the 'leakage PSF' contains about 2% of the total flux of the star and acts as a photometric and astrometric reference for characterisation of the companion's variability and angular separation/orientation with respect to the (often) saturated coronagraphic PSF core.

4. OPTICS AND SIZES

Table of names of optics and locations.
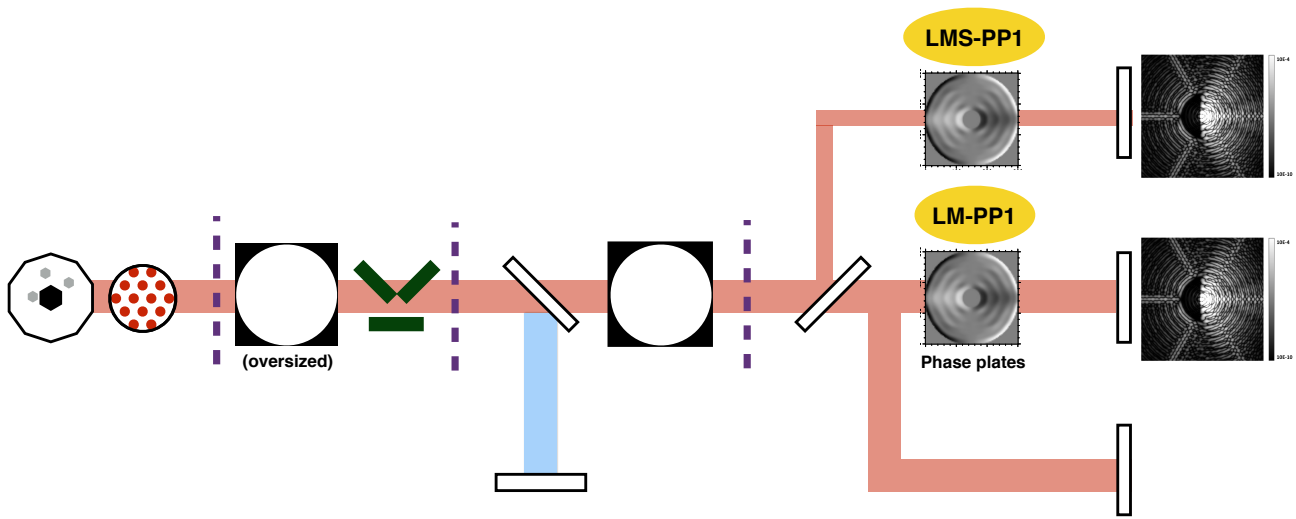
5. NCPA MITIGATION

QACITS and PSI.

Figure 2. The schematic map of METIS showing the location and names of the pupil and focal planes used in HCI, and the names of the optics in the light path.
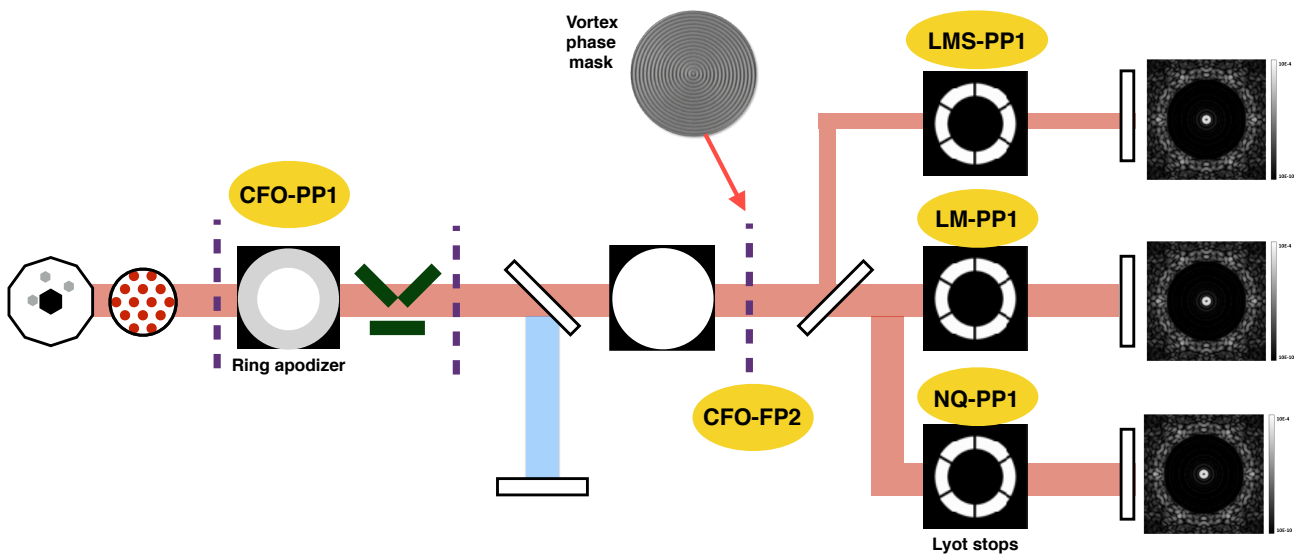

Figure 3. The schematic map of METIS showing the location and names of the pupil and focal planes used in HCI, and the names of the optics in the light path.

6. SIMULATIONS

In order to evaluate realistic high-contrast imaging performance, we simulate an angular differential imaging (ADI) observing sequences in pupil tracking mode, and process the observations with classical ADI (median subtraction) or PCA-ADI algorithms to derive the sensitivity limits. These observations are simulated through an optical propagation routine, using the PROPER library, having as input a set of 6000 residual phase screens generated by the SCAO simulations. They represent only 10 minutes worth of AO residuals in standard conditions on a bright star, while a realistic contrast curve needs to be produced over a longer sequence. For this reason, the short SCAO simulation is artificially turned into a 1 hour observing sequence, by modifying the time sampling (from one screen every 100ms to one screen every 600ms). The performance estimations uses a star transiting at 20 deg from zenith, giving a total parallactic angle rotation of almost 40 deg in one hour.

Using the inputs from METIS simulator, the PROPER simulations are converted into ADU, assuming a target star of magnitude $L = 5$, and the thermal background is added. We multiply the PROPER simulations by the total stellar flux, and add the background emission multiplied by the transmission of all the pupil stops/apodizers in the beam. Photon noise is then added on top of each frame. Classical ADI and PCA-ADI post-processing algorithms are used to process the cubes. The noise radial profile is computed in the final image as the standard deviation of the aperture fluxes measured in as many independent resolution elements as possible at a given angular separation from the star. The noise estimation takes into account the small-sample penalty (Mawet et al. 2014). For the APP, this estimation is done on the clean half of the FoV. The ADI algorithm throughput is evaluated by injecting fake companions at 10 times the noise level using the off-axis PSF as a template, and by comparing their flux in the final image to the injected flux level. The 5-sigma contrast curve is finally obtained by dividing the $5\times$ noise radial profile by the algorithm throughput radial profile and by the aperture photometry of the off-axis star (using an aperture diameter of λ/D). The resultant contrast curve for the RAVC is shown in Figure **??**, along with measured contrast curves extrapolated from current high contrast imaging cameras on 8m class telescopes today.

7. CONCLUSIONS

We have presented the latest optical layout and design for the baseline modes of METIS, and we expect these to remain the same as we work towards Preliminary Design Review in 2019. Remaining tasks for HCI preparation is the addition of realistic Non-Common Path Aberrations (NCPAs) into the simulations, to confirm that we are able to remain within the baseline requirements of the instrument.
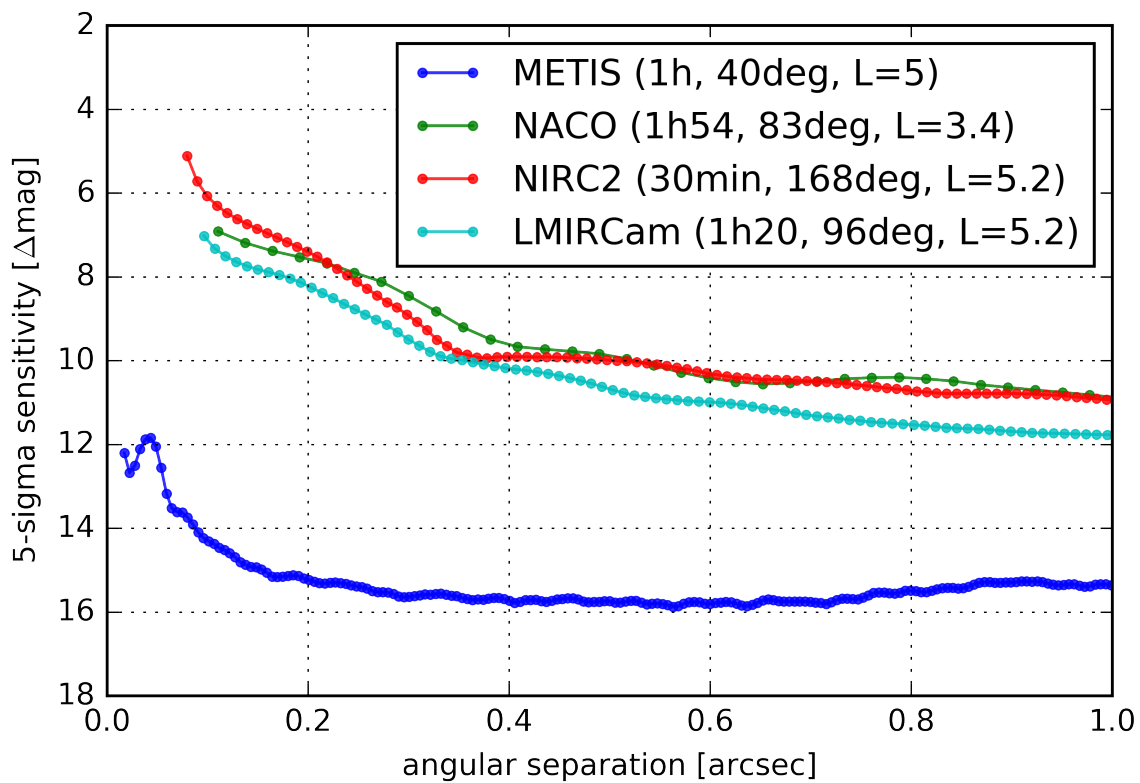
Figure 4. The schematic map of METIS showing the location and names of the pupil and focal planes used in HCI, and the names of the optics in the light path.